

# MambaDETR: Query-based Temporal Modeling using State Space Model for Multi-View 3D Object Detection

Tong Ning

School of Engineering Science  
University of Chinese Academy of Sciences  
Beijing 100049, China  
ningtong22@mails.ucas.ac.cn

Ke Lu

School of Engineering Science  
University of Chinese Academy of Sciences  
Beijing 100049, China  
luk@ucas.ac.cn

Xirui Jiang

School of Engineering Science  
University of Chinese Academy of Sciences  
Beijing 100049, China  
jiangxirui23@mails.ucas.ac.cn

Jian Xue

School of Engineering Science  
University of Chinese Academy of Sciences  
Beijing 100049, China  
xuejian@ucas.ac.cn

## Abstract

*Utilizing temporal information to improve the performance of 3D detection has made great progress recently in the field of autonomous driving. Traditional transformer-based temporal fusion methods suffer from quadratic computational cost and information decay as the length of the frame sequence increases. In this paper, we propose a novel method called MambaDETR, whose main idea is to implement temporal fusion in the efficient state space. Moreover, we design a Motion Elimination module to remove the relatively static objects for temporal fusion. On the standard nuScenes benchmark, our proposed MambaDETR achieves remarkable result in the 3D object detection task, exhibiting state-of-the-art performance among existing temporal*

*fusion methods.*

## 1. Introduction

Multi-view 3D object detection is a fundamental task in autonomous driving, enabling vehicles to perceive their surrounding environment using sensor data. Recent studies have leveraged temporal information from image frame sequences to improve detection performance. Transformers [43] with attention mechanisms have proven effective in modeling dependencies for sequential inputs, leading many approaches to adopt transformer-based temporal fusion methods to explore temporal information for 3D detection.

Existing transformer-based temporal fusion methods,

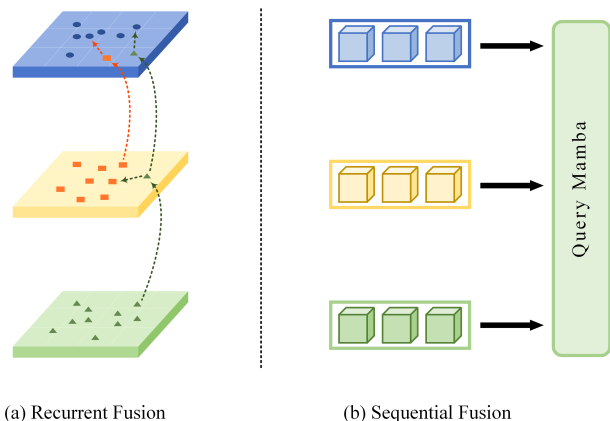


Figure 1. Different temporal fusion methods in recurrent manner and sequential manner.

such as [33, 36], use one adjacent historical frame to interact with the current frame in the transformer decoder, which can efficiently improve 3D detection performance. However, these methods suffer from a quadratic increase in computational cost as the sequence length grows, limiting their ability to adopt more frames for temporal interaction. To solve this problem, subsequent methods [1, 11, 23, 28, 31, 39, 46, 55] incorporate multiple frames into the temporal fusion module by fusing frames in a recurrent (See Figure 1 a) rather than a sequential manner. The long-term historical information is propagated frame by frame, allowing each frame’s features to integrate information from preceding frames. However, this recurrent fusion process can cause information decay over time, leading the model to focus more on current information rather than long-term frame [28, 31].

To address these challenges, we propose a novel method called MambaDETR, which represents temporal fusion candidates as 3D queries initialized from 2D proposals and performs temporal fusion in a hidden space using an SSM-based (Structured State Space Model) module, as shown in Figure 1 (b). This approach replaces the traditional transformer-based module with an SSM-based module, enabling temporal fusion in a sequential manner that effectively models long-range information while maintaining only linear memory and computation costs. Specifically, given a sequence of frames, we first employ a 2D detector to independently generate high-quality 2D proposals for each frame. These proposals are then used to produce 3D object queries through 3D projection, as in previous methods [21], resulting in a sequence of 3D object queries at each time step. Furthermore, according to the physical laws of motion, the same 3D object does not significantly shift between adjacent frames. Therefore, fusing all the queries from the adjacent frames can lead to unnecessary compu-

tational costs. Based on this insight, we introduce a Motion Elimination Module, which aligns the objects from the previous frame to the current frame through ego transformation and generates a motion mask based on the relative movements of objects. Consequently, trivial and relative static objects in the ego vehicle coordinate are removed from the previous frames, retaining only the moving objects and thereby enabling more efficient temporal fusion.

The refined sequence of 3D object queries is then input into the Query Mamba Module, which performs query-based temporal fusion in the state space. By leveraging a structured state space layer, the Query Mamba Module achieves long-range modeling without pairwise comparisons. Consequently, MambaDETR can be efficiently applied to long-range sequences of image frames.

In summary, our contributions include:

- A novel temporal fusion method called MambaDETR is proposed for 3D object detection, which achieves efficient temporal fusion in the state space. This approach sequentially fuses frame sequences, thereby fully exploiting long-range information while avoid quadratic complexity.
- The Motion Elimination module is designed, which removes relatively static objects while retaining moving ones in the ego vehicle coordinates, thereby improving fusion efficiency and reducing computational cost.
- Comprehensive experiments have been conducted on the standard nuScenes dataset, and the evaluation results demonstrate the superior performance of MambaDETR in 3D object detection, with linear computation cost compared to transformer-based methods, e.g. StreamPETR.

## 2. Related Work

### 2.1. Temporal Modeling in Multi-view 3D Object Detection

Multi-view 3D detection is a crucial task in autonomous driving, requiring the processing of multiple camera images and the prediction of 3D bounding boxes. Pioneer’s research [16, 22, 28, 32, 48, 50] centers on the effective conversion of various perspective views into a cohesive 3D space within a single frame. The transformation process can be categorized into two groups: methods based on dense BEV (Bird’s Eye View) representation [13, 16, 22, 27, 28, 30, 35] and methods based on sparse queries [31, 32, 48, 50].

Recent studies [14, 26, 28, 31, 36, 40, 46, 49, 53] have incorporated temporal information to address the occlusion issue and enhance speed prediction accuracy. BEVFormer [28] first introduces sequential temporal modeling into multi-view 3D object detection and applies temporal self-attention. The BEVDet4D [14] paradigm is proposed to be lifted from the spatial-only 3D space to the temporal 4D space. For the first time, vision-based meth-

ods become comparable with those using radar or LiDAR. Sparse4D [31] refines anchor boxes iteratively by incorporating sparse spatial-temporal fusion to improve sparse 3D detection. Additionally, DETR4D [36] introduces a novel hybrid approach that performs cross-frame fusion over past object queries and image features, enabling efficient and robust modeling of temporal information. Recently, StreamPETR [46] efficiently models temporal data and object tracking through frame-by-frame query propagation and motion-aware layer normalization.

## 2.2. State Space Model

State space models have emerged as a promising alternative to traditional sequence modeling approaches. One key issue with traditional attention mechanisms [3, 4, 41, 43], is their quadratic time and space complexity in relation to sequence length. To overcome this limitation, [10] proposed the Linear State-Space Layer (LSSL), a model inspired by control systems that combines recurrent neural networks, temporal convolutions, and neural differential equations. [9] introduced the Structured State Space sequence model (S4), which offers a more efficient computation method while maintaining theoretical strengths for long sequence modeling tasks. Further advancements in state space models include the introduction of the S5 layer [42], exploring the use of Gated State Spaces for long-range language modeling [38]. Recently, the generic language model backbone, Mamba [8], outperforms Transformers at various sizes on large-scale real data and enjoys linear scaling in sequence length. These advancements have been integrated into larger representation models [6, 7, 17, 37, 44], further demonstrating the versatility and scalability of structured state space models in various applications. State space models have also been extended in visual tasks. [18] uses 1D S4 to handle the long-range temporal dependencies for video classification. Trans4mer [19] combines the strengths of S4 and self-attention, achieving state-of-the-art performance for movie scene detection. And VMamba [34] introduces a vision backbone with linear time complexity that integrates Visual State-Space (VSS) blocks with the 2D Selective Scan (SS2D) module.

## 3. Method

Figure 2 illustrates the overall structure of the proposed MambaDETR, which follows the architecture of DETR3D [48], where objects are represented as queries extracted from multi-view image features. MambaDETR develops DETR3D with the following designs: 2D-priors-based query initialization (Section 3.1), Motion Elimination (Section 3.2), and Query Mamba (Section 3.3). For the 2D-priors-based query initialization, we input image features and leverage a 2D detector to obtain 2D proposals. The 3D queries are then initialized from these 2D proposals through

3D projection. The Motion Elimination Module removes redundant, motionless 3D queries from previous frames, retaining only moving 3D queries for temporal fusion. For the Query Mamba, we leverage the 3D query sequence from multiple time steps as input and realize temporal fusion in the state-space. After that, the output queries interact with current image frame in the transformer decoder and generate final 3D prediction.

### 3.1. Query Generator

Previous methods [52] generate numerous queries by applying maximum pooling operations on image heatmaps, which is inefficient and computationally expensive. To address this issue, existing query-based 3D object detection methods [20, 21, 50] have introduced 2D proposals to enhance 3D detection performance. Inspired by these methods, the proposed 2D Priors-based Query Generator uses a 2D object detector to localize objects within specific regions. As a result, the 2D detector not only improves computational efficiency by reducing the number of queries but also provides valuable 2D priors for localizing objects in 3D space. To the best of our knowledge, MambaDETR is the first 3D object detection method that leverages a 2D detector to enhance temporal fusion performance.

Specifically, given the image features after the image backbone, we feed them into the Faster-RCNN detector [50] and a lightweight depth estimation network [27], resulting in a set of 2D bounding boxes and depth distributions. The 2D detector head follows the original design, while the depth distribution is represented in discretized bins [21]. Given each 2D bounding box in view  $i$ , we initialize the 2D query  $\mathbf{Q}_{2D}$  from the center point  $\mathbf{c}_{2D} = (c_w, c_h)$ . To aggregate semantic information of the 2D bounding box, we interact the  $\mathbf{Q}_{2D}$  with the surrounding pixels through deformable attention, following the similar process in [24, 29, 51, 56], to obtain the semantic embedding  $\mathbf{Q}_{sem}$ . The pixel candidates are chosen based on the location of the query and the sampling offsets from the image feature  $\mathbf{F}$  in view  $i$ . The overall process is defined as follows:

$$\begin{aligned} & \text{DeformAttn}(\mathbf{Q}_{2D}, \mathbf{c}_{2D}, \mathbf{F}) \\ &= \sum_{m=1}^{N_{\text{head}}} \mathbf{W}_m \sum_{n=1}^{N_{\text{key}}} A_{mn} \mathbf{W}'_m \mathbf{F}(\mathbf{c}_{2D} + \Delta \mathbf{c}_{mn}), \quad (1) \end{aligned}$$

where  $\mathbf{Q}$ ,  $\mathbf{c}_{2D}$ , and  $\mathbf{F}$  represent the query, reference point, and image features, respectively. The index  $m$  denotes the attention head, and  $N_{\text{head}}$  is the total number of attention heads. The index  $n$  corresponds to the sampled key, and  $N_{\text{key}}$  is the total number of sampled keys for each head.  $A_{mn} \in [0, 1]$  represents the predicted attention weight and  $\mathbf{W}_m, \mathbf{W}'_m$  are the learnable weights. The vector  $\Delta \mathbf{c}_{mn} \in \mathbb{R}^2$  represents the predicted offsets to the reference point

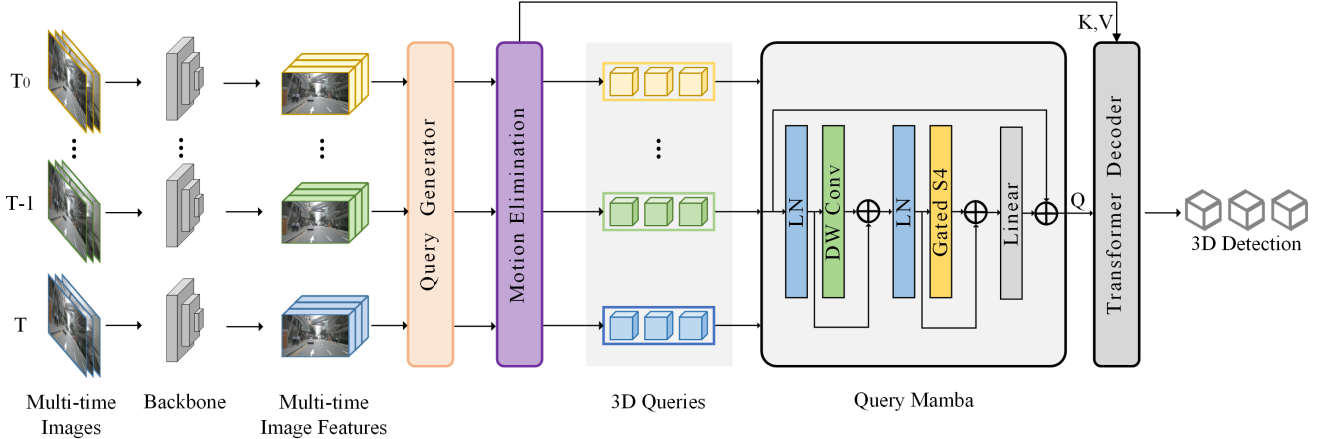


Figure 2. Overall architecture of the proposed MambaDETR. Key enhancements include 2D-priors-based query initialization, Motion Elimination to retain only moving 3D queries across frames, and Query Mamba for state-space temporal fusion. The 3D queries interact with the current image frame in a transformer decoder, producing the final 3D object detections.

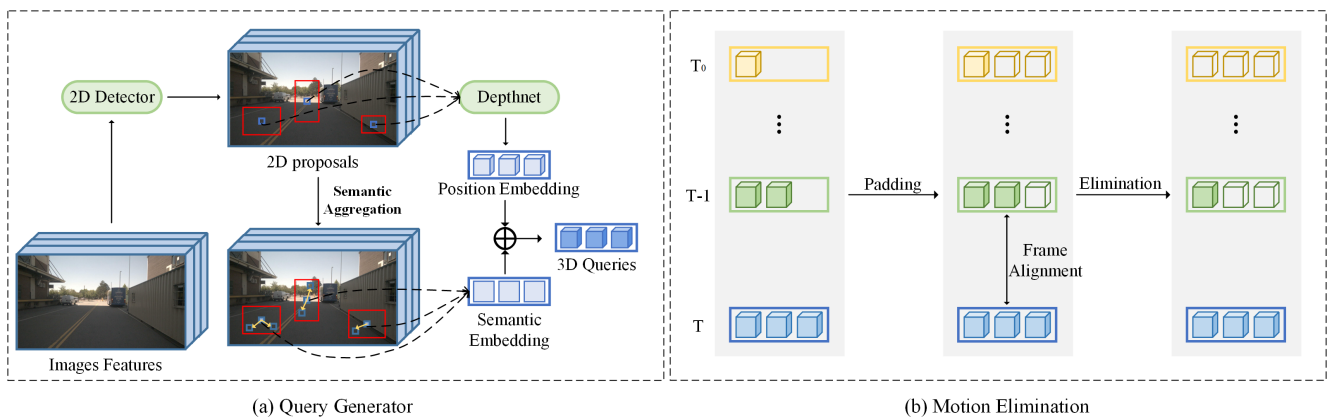


Figure 3. Detail structure of Query Generator and Motion Elimination modules in the MambaDETR architecture. (a) The Query Generator utilizes a 2D detector and DepthNet to create 2D proposals, which are transformed into 3D queries by integrating position and semantic embeddings. (b) The Motion Elimination module then filters out static 3D queries across frames by measuring the distance between the center points.

$\mathbf{c}_{2D}$ . The term  $\mathbf{F}(\mathbf{c}_{2D} + \Delta\mathbf{c}_{mn})$  represents the feature at location  $\mathbf{c}_{2D} + \Delta\mathbf{c}_{mn}$ .

To further lift the 2D query into the 3D space, the center point  $\mathbf{c}_{2D} = (c_w, c_h)$  of each 2d bounding box is combined with the corresponding predicted depth distribution  $\mathbf{d}_c$  and project to the 3D center points  $\mathbf{c}_{3D}$  of 3D proposals:

$$\mathbf{c}_{3D} = \mathbf{K}_j^{-1} \mathbf{I}_j^{-1} [c_w * \mathbf{d}_c, c_h * \mathbf{d}_c, \mathbf{d}_c, \mathbf{1}]^T, \quad (2)$$

where  $\mathbf{K}_j$ ,  $\mathbf{I}_j$  denote extrinsic and intrinsic matrices of the  $j$ -th camera.

After generating center points  $\mathbf{c}_{3D}$  of the 3D proposals, we use sinusoidal transformation and MLP to obtain the 3D position embedding  $\mathbf{Q}_{\text{pos}}$  following the process and combine with the aforementioned  $\mathbf{Q}_{\text{sem}}$  together and result in

3D query  $\mathbf{Q}_{3D}$ :

$$\begin{aligned} \mathbf{Q}_{\text{pos}} &= \text{PosEmbed}(\mathbf{c}_{3D}), \\ \mathbf{Q}_{3D} &= \mathbf{Q}_{\text{pos}} + \mathbf{Q}_{\text{sem}}. \end{aligned} \quad (3)$$

### 3.2. Motion Elimination

The Motion Elimination (ME) module is applied optimize the computation cost by discarding the relative static object queries for the subsequent temporal fusion. In more detail, we present the structure of ME module in Figure 3b, which consists of three parts: zero padding, frame alignment. For the zero padding part, given the 3D queries sequence  $\mathbf{Q}_{3D}^{\text{seq}} = [\mathbf{Q}_{3D}^t, \mathbf{Q}_{3D}^{t-1}, \dots, \mathbf{Q}_{3D}^{t-N}]$ , we select the 3D queries with the in the  $i$ -th frame  $\mathbf{Q}_{3D}^i$  that have the largest number of 3D proposal and represented as  $K$ .

Then we add zero padding to all the 3D queries in the remaining frames and get the updated 3D queries sequence  $\hat{\mathbf{Q}}_{3D}^{\text{seq}} = [\hat{\mathbf{Q}}_{3D}^t, \hat{\mathbf{Q}}_{3D}^{t-1}, \dots, \hat{\mathbf{Q}}_{3D}^{t-N}]$  with size of  $K \times N$ .

For the frame alignment, we select the current queries  $\hat{\mathbf{Q}}_{3D}^t$ , previous queries in the  $t-j$  frame  $\hat{\mathbf{Q}}_{3D}^{t-j}$  and their corresponding 3D center points  $\mathbf{C}_{3D}^t, \mathbf{C}_{3D}^{t-j}$ . Then the previous query  $\hat{\mathbf{Q}}_{3D}^{t-j}$  is aligned to the current frame through ego transformation, which following the process in [12]. Given the ego pose matrix of  $\mathbf{R}_w^t$  and  $\mathbf{R}_w^{t-j}$  in the current and  $t-j$  frame, we first compute the ego transformation matrix and align the center of the objects in the  $t-j$  frame to the current frame. The overall process is formulated as:

$$\begin{aligned} \mathbf{R}_{t-j}^t &= \mathbf{R}_w^t \cdot \text{inv}(\mathbf{R}_w^{t-j}), \\ \mathbf{C}_{t-1}' &= (\mathbf{C}_{t-1} + \mathbf{V}_{t-j} \cdot \Delta t) \cdot (\mathbf{R}_{t-j}^t)^T. \end{aligned} \quad (4)$$

After getting the aligned center points, we utilize the L2 center distance of object and create cost matrix  $\mathbf{D}_{t-j}^t \in \mathbb{R}^{K \times K}$  to measure the moving distance of objects between the chosen frames.

$$\mathbf{D}_{t-j}^t = \mathbf{L}_2(\mathbf{C}_t - \mathbf{C}_{t-1}') \quad (5)$$

Then we distinguish the relative static position of the objects with two standards: The L2 distance of object is below the threshold  $\alpha$  and the category of the objects in frame  $t$  and  $t-j$  are the same.

$$\begin{aligned} \mathbf{M}_{t-j} &= \begin{cases} 0, & D_{t-j}^t \leq \alpha \text{ and } \text{CAT}_t = \text{CAT}_{t-j} \\ 1e^6, & D_{t-j}^t > \alpha \text{ or } \text{CAT}_t \neq \text{CAT}_{t-j} \end{cases}, \\ \mathbf{A}_{t-j} &= \text{softmax}(\mathbf{M}_{t-j}), \end{aligned} \quad (6)$$

where  $\mathbf{A}_{t-j} \in \mathbb{R}^{K \times K}$ . We identify the object of  $t-j$  frame is relative static if it has one relative static relationship in the  $t$  frame. The process is formulated as:

$$B_j^n = \begin{cases} 1 & \text{if } \sum_{m=1}^K \mathbf{A}_{t-j}^{mn} = K \\ 0 & \text{otherwise} \end{cases}. \quad (7)$$

After that, we can obtain the motion mask of the  $t-j$  frame  $\mathbf{B}_{t-j} = \{B_{t-j}^n\}_{n=1}^K \in \mathbb{R}^{1 \times K}$ . We extend the above process to all the previous frames and gather the motion mask  $\mathbf{B} = [\mathbf{B}_t^T, \mathbf{B}_{t-1}^T, \dots, \mathbf{B}_{t-N}^T]$ . To be notice that we set all the elements of  $\mathbf{B}_t$  to be 1, which means all the queries of the current frame will be remained. Finally, we multiply the 3D queries sequence with the motion mask and get the relative moving query sequence:

$$\begin{aligned} \mathbf{Q}_{\text{moving}} &= \hat{\mathbf{Q}}_{3D}^{\text{seq}} * \mathbf{B} \\ &= [\hat{\mathbf{Q}}_{3D}^t, \hat{\mathbf{Q}}_{3D}^{t-1}, \dots, \hat{\mathbf{Q}}_{3D}^{t-N}] * [\mathbf{B}_t^T, \mathbf{B}_{t-1}^T, \dots, \mathbf{B}_{t-N}^T]. \end{aligned} \quad (8)$$

### 3.3. Query Mamba

#### 3.3.1 Background

The Structured State-Space Model (SSM) can be regarded as linear-time-invariant system that map the input stimulation  $x(t)$  to the response  $y(t)$  through the hidden state  $h(t) \in \mathbb{R}^N$ . The SSM can be defined in the continuous time using the following equations:

$$\begin{aligned} \mathbf{h}'(t) &= \mathbf{A}\mathbf{h}(t) + \mathbf{B}x(t), \\ y(t) &= \mathbf{C}\mathbf{h}(t) + Dx(t), \end{aligned} \quad (9)$$

where  $\mathbf{A} \in \mathbb{R}^{N \times N}$ ,  $\mathbf{B} \in \mathbb{R}^{N \times 1}$ ,  $\mathbf{C} \in \mathbb{R}^{1 \times N}$  and  $D \in \mathbb{R}^1$  are the weighting parameters.

To apply the continuous SSM into the deep models, we introduce a timescale parameter  $\Delta$  and discretize the SSM as follow:

$$\begin{aligned} \mathbf{h}_k &= \bar{\mathbf{A}}\mathbf{h}_{k-1} + \bar{\mathbf{B}}\mathbf{x}_k, \\ y_k &= \bar{\mathbf{C}}\mathbf{h}_k + \bar{D}\mathbf{x}_k, \end{aligned} \quad (10)$$

where  $\bar{\mathbf{A}}, \bar{\mathbf{B}}, \bar{\mathbf{C}}$  and  $\bar{D}$  are the discrete version of  $\mathbf{A}, \mathbf{B}, \mathbf{C}$  and  $D$ . The equation (10) can also be expressed as a convolution operation:

$$\begin{aligned} \bar{\mathbf{K}} &= (\bar{\mathbf{C}}\bar{\mathbf{B}}, \bar{\mathbf{C}}\bar{\mathbf{A}}\bar{\mathbf{B}}, \dots, \bar{\mathbf{C}}\bar{\mathbf{A}}^{L-1}\bar{\mathbf{B}}), \\ \mathbf{y} &= \bar{\mathbf{K}} * \mathbf{x}, \end{aligned} \quad (11)$$

where  $\bar{\mathbf{K}}$  is convolution kernel and  $L$  is the length of the input sequence.

#### 3.3.2 Query Mamba

The overview of the proposed Query Mamba is shown in Figure 2. For the queries  $\hat{\mathbf{Q}}_{3D}^{t-i}$  in the  $t-i$  frame, we concatenate all the queries along the channel dimension  $D$  and get the fusion candidate  $\mathbf{Q}_{\text{moving}}^{t-i} \in \mathbb{R}^{1 \times KD}$ . After that, following the standard 1-D input of Mamba, we send the fusion candidate sequence  $\mathbf{Q}_{\text{moving}} = \{\mathbf{Q}_{\text{moving}}^{t-i}\}_{i=1}^N \in \mathbb{R}^{N \times KD}$  into the Query Mamba module.

First, we pass the sequence through the Layer Normalization layer. Subsequently, we apply a depth-wise convolution (DW Conv) along with a residual connection, which improves the efficiency of the CNN and has been used in VMamba [34]. Afterward, we apply another Layer Normalization and a Gated S4 (GS4) layer, also with a residual connection. Finally, the sequence is passed through a Linear layer with a residual connection that connects from the initial input of Query Mamba:

$$\begin{aligned} \mathbf{z} &= \text{DWConv}(\text{LN}(\mathbf{Q}_{\text{moving}})) + \text{LN}(\mathbf{Q}_{\text{moving}}), \\ \mathbf{z}' &= \text{GS4}(\text{LN}(\mathbf{z})) + \text{LN}(\mathbf{z}), \\ \mathbf{Q}_{\text{out}} &= \text{Linear}(\mathbf{z}') + \mathbf{Q}_{\text{moving}}. \end{aligned}$$

The SSM-based model plays a vital role in our Mamba DETR method, so as the cross-attention in the transformer-based temporal fusion methods [28, 46]. Given the input sequence  $\mathbf{Q}_{\text{moving}} = \{\mathbf{Q}_{\text{moving}}^{t-i}\}_{i=1}^N \in \mathbb{R}^{N \times KD}$ , the computational complexity of cross-attention and SSM is formulated as:

$$\begin{aligned}\Omega(\text{cross-attention}) &= 4N(KD)^2 + 2N^2KD, \\ \Omega(\text{SSM}) &= 3N(2D)M + N(2KD)M,\end{aligned}$$

where  $M$  is a fixed parameter set to 16. As we can see, the computational complexity of cross-attention is quadratic in the sequence length  $N$ , while the SSM is linear in  $N$ . This computational advantage makes the SSM-based method scalable for long sequence modeling and thus beneficial for long-range exploration.

## 4. Experiments

Table 1. Ablation study on different components of MambaDETR

2D detector	SE	ME	QMamba	NDS	mAP
×	×	×	×	57.5	49.4
✓	×	×	×	58.1	49.8
✓	✓	×	×	58.3	50.4
✓	✓	✓	×	58.6	50.5
✓	✓	✓	✓	<b>60.5</b>	<b>50.8</b>

Table 2. Ablation Study on the Computational Efficiency of the 2D Detector and Motion Elimination

2D Detector	ME	FPS	Memory (GB)
×	×	30.4	16.0
✓	×	29.7	16.1
✓	✓	<b>31.9</b>	<b>15.5</b>

Table 3. S4 variants

S4 variant	mAP
S4	50.1
S6	50.3
DS4	<b>50.8</b>
GS6	49.4

Table 4. Number of layers

S4 layers	mAP
1	49.1
2	49.7
4	50.5
6	<b>50.8</b>

### 4.1. Dataset and Metrics

The nuScenes dataset is a comprehensive resource for 3D object detection, encompassing 1,000 scenes, each lasting about 20 seconds and annotated at a frequency of 2 Hz. This dataset features images captured from six cameras, alongside data from five radars and one LiDAR system, providing a complete 360° field of view. The annotations include

up to 1.4 million 3D bounding boxes across ten categories: car, truck, bus, trailer, construction vehicle, pedestrian, motorcycle, bicycle, barrier, and traffic cone. The scenes are organized into training (700), validation (150), and testing (150) sets. For evaluation, we utilize several metrics, including the mean Average Precision (mAP), nuScenes Detection Score (NDS), and various True Positive metrics such as Average Translation Error (ATE) and Average Velocity Error (AVE). The mAP is determined based on the distance between 2D centers on the ground plane, and NDS provides a holistic measure of detection performance by aggregating other relevant indicators.

## 4.2. Ablation Study

### 4.2.1 2D Detector and Semantic aggregation

We analyze the impact of the 2D detector and the Semantic Aggregation (SE) module on generating object queries, as shown in Table 1 and Table 2. Specifically, adding the 2D detector for query generation achieves significant improvements, with mAP increasing by 0.6% and NDS increasing by 0.4%. This result indicates that the 2D detector can provide reliable 2D priors for the query generator and thus benefit 3D object detection. Besides, it can also be seen that the 2D detector negatively impacts inference speed and GPU memory usage. We argue that the additional computational cost introduced by the 2D detector outweighs the savings from the reduced number of queries. Semantic aggregation is also proven to be effective in improving the quality of queries, indicating the importance of semantic information in query generation.

### 4.2.2 Motion Elimination

MambaDETR reduces the non-trivial queries through the Motion Elimination (ME) module. Table 2 shows that the ME module can significantly improve inference speed by 1.2 FPS and reduce GPU memory usage by 0.6 GB, which indicates that the ME module successfully removes the non-vital queries. Furthermore, the proposed ME module also achieves a limited improvement of 0.1% in mAP and 0.3% in NDS. This indicates that reducing redundant queries can not only improve computational efficiency but also benefit detection performance.

### 4.2.3 Query Mamba

We experiment with different S4 variants (Table 3) and the impact of varying the number of layers (Table 4). In Table 3, we evaluate several S4 variants, including the standard S4, S6, Diagonal S4 (DS4), and Gated S4 (GS4). Our findings indicate that GS6 achieves the highest mAP of 50.8, outperforming the other variants. In Table 4, we assess the

Table 5. Comparison with existing methods on nuScenes *validation* set.

	Backbone	Frames	NDS $\uparrow$	mAP $\uparrow$	mATE $\downarrow$	mASE $\downarrow$	mAOE $\downarrow$	mAVE $\downarrow$	mAAE $\downarrow$
BEVDet [16]	ResNet50	1	37.9	29.8	72.5	27.9	58.9	86.0	24.5
BEVDet4D [14]	ResNet50	2	45.7	32.2	70.3	27.8	49.5	35.4	20.6
PETrv2 [33]	ResNet50	2	45.6	34.9	70.0	27.5	58.0	43.7	18.7
BEVDepth [27]	ResNet50	2	47.5	35.1	63.9	26.7	47.9	42.8	19.8
BEVStereo [26]	ResNet50	2	50.0	37.2	59.8	27.0	43.8	36.7	19.0
BEVFormer v2 [54]	ResNet50	-	52.9	42.3	61.8	27.3	41.3	33.3	18.8
SOLOFusion [40]	ResNet50	16+1	53.4	42.7	56.7	27.4	51.1	25.2	18.1
BEVPoolv2 [15]	ResNet50	8+1	52.6	40.6	57.2	27.5	46.3	27.5	18.8
StreamPETR [46]	ResNet50	8	55.0	45.0	61.3	26.7	41.3	26.5	19.6
DETR3D [48]	ResNet101-DCN	1	43.4	34.9	71.6	26.8	37.9	84.2	20.0
Focal-PETR [45]	ResNet101-DCN	1	46.1	39.0	67.8	26.3	39.5	80.4	20.2
PETR [32]	ResNet101-DCN	1	44.1	36.6	71.7	26.7	41.2	83.4	19.0
BEVFormer [28]	ResNet101-DCN	4	51.7	41.6	67.3	27.4	37.2	39.4	19.8
PolarDETR [2]	ResNet101-DCN	2	48.8	38.3	70.7	26.9	34.4	51.8	19.6
Sparse4D [31]	ResNet101-DCN	4	54.1	43.6	63.3	27.9	36.3	31.7	17.7
BEVDepth [27]	ResNet101	2	53.5	41.2	56.5	26.6	35.8	33.1	19.0
SOLOFusion [40]	ResNet101	16+1	58.2	48.3	<b>50.3</b>	26.4	38.1	24.6	20.7
StreamPETR [46]	ResNet101	8	59.2	50.4	56.9	<b>26.2</b>	31.5	25.7	19.9
MambaDETR	ResNet101	8	<b>60.5</b>	<b>50.8</b>	53.7	26.4	<b>30.7</b>	<b>24.4</b>	<b>17.2</b>

Table 6. Comparison with existing methods on nuScenes *test* set.

	Backbone	NDS $\uparrow$	mAP $\uparrow$	mATE $\downarrow$	mASE $\downarrow$	mAOE $\downarrow$	mAVE $\downarrow$	mAAE $\downarrow$
FCOS3D [47]	R101-DCN	35.8	42.8	69.0	24.9	45.2	143.4	12.4
DETR3D [48]	V2-99	41.2	47.9	64.1	25.5	39.4	84.5	13.3
MV2D [50]	V2-99	46.3	51.4	54.2	24.7	40.3	85.7	12.7
UVTR [25]	V2-99	47.2	55.1	57.7	25.3	39.1	50.8	12.3
BEVFormer [28]	V2-99	48.1	56.9	58.2	25.6	37.5	37.8	12.6
PETrv2 [33]	V2-99	49.0	58.2	56.1	24.3	36.1	34.3	12.0
PolarFormer [22]	V2-99	49.3	57.2	55.6	25.6	30.4	43.9	12.7
BEVStereo [26]	V2-99	52.5	61.0	<b>43.1</b>	24.6	35.8	35.7	13.8
StreamPETR [46]	V2-99	55.0	63.6	47.9	23.9	31.7	24.1	11.9
BEVDet4D [14]	Swin-B [32]	45.1	56.9	51.1	24.1	38.6	30.1	<b>12.1</b>
BEVDepth [27]	ConvNeXt-B	52.0	60.9	44.5	24.3	35.2	34.7	12.7
AeDet [5]	ConvNeXt-B	53.1	62.0	43.9	24.7	34.4	29.2	13.0
PETrv2 [33]	RevCol-L [3]	51.2	59.2	54.7	24.2	36.0	36.7	12.6
SOLOFusion [40]	ConvNeXt-B	54.0	61.9	45.3	25.7	37.6	27.6	14.8
StreamPETR [46]	ViT-L [9]	<b>62.0</b>	67.6	47.0	24.1	<b>25.8</b>	23.6	13.4
MambaDETR	ViT-L [9]	60.7	<b>68.2</b>	48.1	<b>23.9</b>	26.1	<b>22.8</b>	12.7

effect of increasing the number of S4 layers on mAP. The results demonstrate that performance improves steadily with additional layers, stabilizing at an mAP of 50.8 with 6 layers. The result indicates that GS4 model with 6 layer can achieve the best performance.

### 4.3. Results and Analysis

#### 4.3.1 Main Results

We compare the proposed Mamba DETR with previous state-of-the-art vision-based 3D detectors on the nuScenes validation and test sets. As shown in Table 5, Mamba DETR demonstrates superior performance on the validation set, achieving significant improvements in NDS, mAP, and localization metrics compared to other methods. Specifically, with a ResNet101 backbone and 8-frame input, Mamba

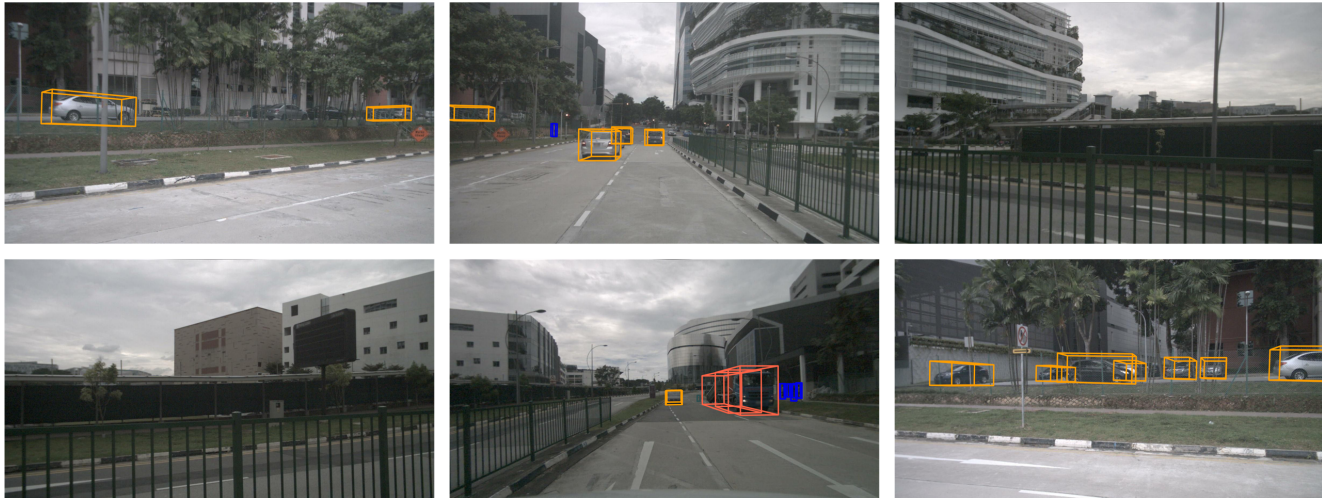


Figure 4. Visualization of MambaDETR.

DETR outperforms StreamPETR by 0.7% in NDS and 0.4% in mAP. The mATE value of Mamba DETR also shows notable improvements, reducing the localization error compared to most competitors. This indicates the efficacy of Mamba DETR’s object detection and tracking capabilities.

When comparing the performance on the test set in Table 6, Mamba DETR again achieves impressive results. With a ViT-Large backbone, Mamba DETR reaches an mAP of 68.2% and an NDS of 60.7%, surpassing StreamPETR by 0.6% in mAP and demonstrating comparable performance in mASE and mAOE metrics. Notably, Mamba DETR also achieves lower mAVE compared to many competing methods, suggesting improved velocity estimation and better temporal consistency for tracking moving objects. Besides, we show the visualization of the detection results In Figure 4, which also effectively demonstrate the superior performance of the proposed MambaDETR.

### 4.3.2 Temporal Extent Analysis

To validate long-term exploration of input image sequence, we evaluate both StreamPETR and MambaDETR with different numbers of training frames (i.e., 1, 2, 4, 8, and 12). The results are presented in Figure 5 (a). First, we notice that a short temporal window of 2 training frames produces a suboptimal performance of 40.7% mAP. Expanding the temporal range to 8 frames boosts the performance to 50.8% mAP, reflecting a 10.1% improvement. Extending further to 12 frames continues to enhance the mAP, reaching 52.2%, which indicates that adding more frames does not obtain promising improvements. Compared to our baseline, StreamPETR, MambaDETR consistently outperforms in terms of mAP across all training frames, particularly excelling with an extended temporal window. This demon-

strates the superior capability of our proposed method to leverage long-range temporal information, resulting in significantly better detection performance.

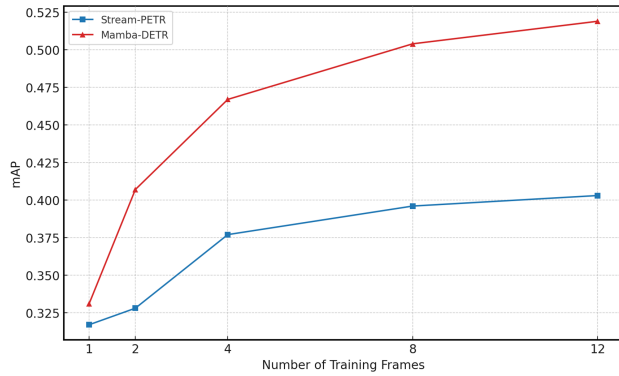
### 4.3.3 Computational Efficiency Analysis

In Figure 5b and c, we analyze the computational efficiency of the MambaDETR in two aspect: inference speed and memory cost. In Figure 5b, we observe that the inference speed decreases as the sequence length increase from 35.9% to 26.0% in FPS. Meanwhile, the inference speed of StreamPETR remains stable around 27% due to the recurrent temporal fusion mechanism that keep the fusion candidates invariant to the sequence length. However, our MambaDETR still infer faster than StreamPETR except for the frame numbers equal to 12. Moreover, Figure 5c demonstrates that MambaDETR has significantly lower memory consumption compared to StreamPETR, with only linear memory increase as the sequence length grow. With 12 frames, MambaDETR requires around 15 GB of memory, whereas StreamPETR’s memory requirement is considerably higher, peaking at nearly 40 GB.

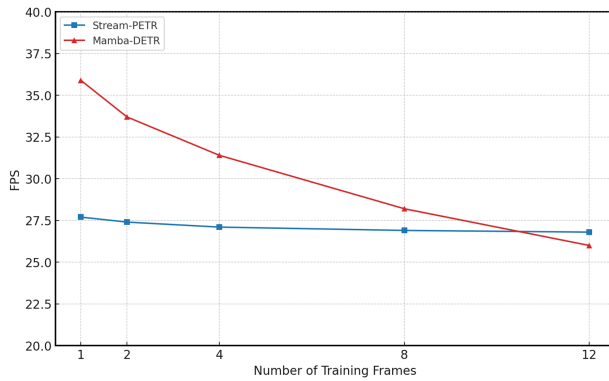
## 5. Conclusion

In this paper, we propose MambaDETR, an effective 3D object detection framework for long-sequence temporal fusion. Unlike previous approaches, our method uses a state-space model (SSM) to perform efficient, sequential temporal fusion with linear memory and computational complexity. Additionally, we introduce the Motion Elimination Module, which selectively retains only moving objects, enhancing fusion efficiency. MambaDETR achieves state-of-the-art performance on the nuScenes dataset, demonstrating significant improvements in computational efficiency

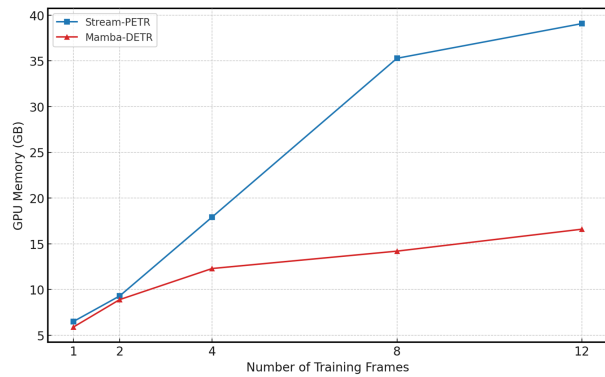




(a) Performance



(b) Inference Speed



(c) Memory Requirement

Figure 5. Performance(mAP), Inference Speed(samples/Second) and Memory Requirements(GB) of MambaDETR as the function of the sequence length.

over transformer-based methods while maintaining accuracy. We hope MambaDETR offers valuable insights for advancing long-sequence temporal modeling in autonomous driving applications.

## References

- [1] Jiarui Cai, Mingze Xu, Wei Li, Yuanjun Xiong, Wei Xia, Zhuowen Tu, and Stefano Soatto. Memot: Multi-object tracking with memory. In *Proceedings of the IEEE/CVF Conference on Computer Vision and Pattern Recognition*, pages 8090–8100, 2022. 2
- [2] Shaoyu Chen, Xinggang Wang, Tianheng Cheng, Qian Zhang, Chang Huang, and Wenyu Liu. Polar parametrization for vision-based surround-view 3d detection. *arXiv preprint arXiv:2206.10965*, 2022. 7
- [3] Tri Dao. Flashattention-2: Faster attention with better parallelism and work partitioning. *arXiv preprint arXiv:2307.08691*, 2023. 3
- [4] Tri Dao, Dan Fu, Stefano Ermon, Atri Rudra, and Christopher Ré. Flashattention: Fast and memory-efficient exact attention with io-awareness. *Advances in Neural Information Processing Systems*, 35:16344–16359, 2022. 3
- [5] Chengjian Feng, Zequn Jie, Yujie Zhong, Xiangxiang Chu, and Lin Ma. Aedet: Azimuth-invariant multi-view 3d object detection. In *Proceedings of the IEEE/CVF Conference on Computer Vision and Pattern Recognition*, pages 21580–21588, 2023. 7
- [6] Daniel Y Fu, Tri Dao, Khaled K Saab, Armin W Thomas, Atri Rudra, and Christopher Ré. Hungry hungry hippos: Towards language modeling with state space models. *arXiv preprint arXiv:2212.14052*, 2022. 3
- [7] Karan Goel, Albert Gu, Chris Donahue, and Christopher Ré. It’s raw! audio generation with state-space models. In *International Conference on Machine Learning*, pages 7616–7633, 2022. 3
- [8] Albert Gu and Tri Dao. Mamba: Linear-time sequence modeling with selective state spaces. *arXiv preprint arXiv:2312.00752*, 2023. 3
- [9] Albert Gu, Karan Goel, and Christopher Ré. Efficiently modeling long sequences with structured state spaces. *arXiv preprint arXiv:2111.00396*, 2021. 3
- [10] Albert Gu, Isys Johnson, Karan Goel, Khaled Saab, Tri Dao, Atri Rudra, and Christopher Ré. Combining recurrent, convolutional, and continuous-time models with linear state space layers. *Advances in neural information processing systems*, 34:572–585, 2021. 3
- [11] Fei He, Naiyu Gao, Jian Jia, Xin Zhao, and Kaiqi Huang. Queryprop: Object query propagation for high-performance video object detection. In *Proceedings of the AAAI Conference on Artificial Intelligence*, pages 834–842, 2022. 2
- [12] Jinghua Hou, Zhe Liu, Zhikang Zou, Xiaoqing Ye, Xiang Bai, et al. Query-based temporal fusion with explicit motion for 3d object detection. *Advances in Neural Information Processing Systems*, 36, 2024. 5
- [13] Bin Huang, Yangguang Li, Enze Xie, Feng Liang, Luya Wang, Mingzhu Shen, Fenggang Liu, Tianqi Wang, Ping Luo, and Jing Shao. Fast-bev: Towards real-time on-vehicle bird’s-eye view perception. *arXiv preprint arXiv:2301.07870*, 2023. 2
- [14] Junjie Huang and Guan Huang. Bevdet4d: Exploit temporal cues in multi-camera 3d object detection. *arXiv preprint arXiv:2203.17054*, 2022. 2, 7

- [15] Junjie Huang and Guan Huang. Bevpoolv2: A cutting-edge implementation of bevdet toward deployment. *arXiv preprint arXiv:2211.17111*, 2022. 7
- [16] Junjie Huang, Guan Huang, Zheng Zhu, Yun Ye, and Dalong Du. Bevdet: High-performance multi-camera 3d object detection in bird-eye-view. *arXiv preprint arXiv:2112.11790*, 2021. 2, 7
- [17] Tao Huang, Xiaohuan Pei, Shan You, Fei Wang, Chen Qian, and Chang Xu. Localmamba: Visual state space model with windowed selective scan. *arXiv preprint arXiv:2403.09338*, 2024. 3
- [18] Md Mohaiminul Islam and Gedas Bertasius. Long movie clip classification with state-space video models. In *European Conference on Computer Vision*, pages 87–104. Springer, 2022. 3
- [19] Md Mohaiminul Islam, Mahmudul Hasan, Kishan Shamsundar Athrey, Tony Braskich, and Gedas Bertasius. Efficient movie scene detection using state-space transformers. In *Proceedings of the IEEE/CVF Conference on Computer Vision and Pattern Recognition*, pages 18749–18758, 2023. 3
- [20] Haoxuanye Ji, Pengpeng Liang, and Erkang Cheng. Enhancing 3d object detection with 2d detection-guided query anchors. In *Proceedings of the IEEE/CVF Conference on Computer Vision and Pattern Recognition*, pages 21178–21187, 2024. 3
- [21] Xiaohui Jiang, Shuailin Li, Yingfei Liu, Shihao Wang, Fan Jia, Tiancai Wang, Lijin Han, and Xiangyu Zhang. Far3d: Expanding the horizon for surround-view 3d object detection. In *Proceedings of the AAAI Conference on Artificial Intelligence*, pages 2561–2569, 2024. 2, 3
- [22] Yanqin Jiang, Li Zhang, Zhenwei Miao, Xiatian Zhu, Jin Gao, Weiming Hu, and Yu-Gang Jiang. Polarformer: Multi-camera 3d object detection with polar transformer. In *Proceedings of the AAAI conference on Artificial Intelligence*, pages 1042–1050, 2023. 2, 7
- [23] Zhengkai Jiang, Peng Gao, Chaoxu Guo, Qian Zhang, Shiming Xiang, and Chunhong Pan. Video object detection with locally-weighted deformable neighbors. In *Proceedings of the AAAI Conference on Artificial Intelligence*, pages 8529–8536, 2019. 2
- [24] Hongyang Li, Hao Zhang, Zhaoyang Zeng, Shilong Liu, Feng Li, Tianhe Ren, and Lei Zhang. Dfa3d: 3d deformable attention for 2d-to-3d feature lifting. In *Proceedings of the IEEE/CVF International Conference on Computer Vision*, pages 6684–6693, 2023. 3
- [25] Yanwei Li, Yilun Chen, Xiaojuan Qi, Zeming Li, Jian Sun, and Jiaya Jia. Unifying voxel-based representation with transformer for 3d object detection. *Advances in Neural Information Processing Systems*, 35:18442–18455, 2022. 7
- [26] Yinhao Li, Han Bao, Zheng Ge, Jinrong Yang, Jianjian Sun, and Zeming Li. Bevestereo: Enhancing depth estimation in multi-view 3d object detection with temporal stereo. In *Proceedings of the AAAI Conference on Artificial Intelligence*, pages 1486–1494, 2023. 2, 7
- [27] Yinhao Li, Zheng Ge, Guanyi Yu, Jinrong Yang, Zengran Wang, Yukang Shi, Jianjian Sun, and Zeming Li. Bevdepth: Acquisition of reliable depth for multi-view 3d object detection. In *Proceedings of the AAAI Conference on Artificial Intelligence*, pages 1477–1485, 2023. 2, 3, 7
- [28] Zhiqi Li, Wenhai Wang, Hongyang Li, Enze Xie, Chonghao Sima, Tong Lu, Yu Qiao, and Jifeng Dai. Bevformer: Learning bird’s-eye-view representation from multi-camera images via spatiotemporal transformers. In *European conference on computer vision*, pages 1–18. Springer, 2022. 2, 6, 7
- [29] Jingyun Liang, Yuchen Fan, Xiaoyu Xiang, Rakesh Ranjan, Eddy Ilg, Simon Green, Jiezhong Cao, Kai Zhang, Radu Timofte, and Luc V Gool. Recurrent video restoration transformer with guided deformable attention. *Advances in Neural Information Processing Systems*, 35:378–393, 2022. 3
- [30] Tingting Liang, Hongwei Xie, Kaicheng Yu, Zhongyu Xia, Zhiwei Lin, Yongtao Wang, Tao Tang, Bing Wang, and Zhi Tang. Bevfusion: A simple and robust lidar-camera fusion framework. *Advances in Neural Information Processing Systems*, 35:10421–10434, 2022. 2
- [31] Xuewu Lin, Tianwei Lin, Zixiang Pei, Lichao Huang, and Zhizhong Su. Sparse4d: Multi-view 3d object detection with sparse spatial-temporal fusion. *arXiv preprint arXiv:2211.10581*, 2022. 2, 3, 7
- [32] Yingfei Liu, Tiancai Wang, Xiangyu Zhang, and Jian Sun. Petr: Position embedding transformation for multi-view 3d object detection. In *European Conference on Computer Vision*, pages 531–548, 2022. 2, 7
- [33] Yingfei Liu, Junjie Yan, Fan Jia, Shuailin Li, Aqi Gao, Tiancai Wang, and Xiangyu Zhang. Petr2: A unified framework for 3d perception from multi-camera images. In *Proceedings of the IEEE/CVF International Conference on Computer Vision*, pages 3262–3272, 2023. 2, 7
- [34] Y Liu, Y Tian, Y Zhao, H Yu, L Xie, Y Wang, Q Ye, and Y Liu. Vmamba: Visual state space model. *arXiv preprint arXiv:2401.10166*, 2024. 3, 5
- [35] Zhijian Liu, Haotian Tang, Alexander Amini, Xinyu Yang, Huizi Mao, Daniela L Rus, and Song Han. Bevfusion: Multi-task multi-sensor fusion with unified bird’s-eye view representation. In *2023 IEEE international conference on robotics and automation (ICRA)*, pages 2774–2781. IEEE, 2023. 2
- [36] Zhipeng Luo, Changqing Zhou, Gongjie Zhang, and Shijian Lu. Detr4d: Direct multi-view 3d object detection with sparse attention. *arXiv preprint arXiv:2212.07849*, 2022. 2, 3
- [37] Xuezhe Ma, Chunting Zhou, Xiang Kong, Junxian He, Liangke Gui, Graham Neubig, Jonathan May, and Luke Zettlemoyer. Mega: moving average equipped gated attention. *arXiv preprint arXiv:2209.10655*, 2022. 3
- [38] Harsh Mehta, Ankit Gupta, Ashok Cutkosky, and Behnam Neyshabur. Long range language modeling via gated state spaces. *arXiv preprint arXiv:2206.13947*, 2022. 3
- [39] Tim Meinhardt, Alexander Kirillov, Laura Leal-Taixe, and Christoph Feichtenhofer. Trackformer: Multi-object tracking with transformers. In *Proceedings of the IEEE/CVF conference on computer vision and pattern recognition*, pages 8844–8854, 2022. 2
- [40] Jinhyung Park, Chenfeng Xu, Shijia Yang, Kurt Keutzer, Kris Kitani, Masayoshi Tomizuka, and Wei Zhan. Time will

- tell: New outlooks and a baseline for temporal multi-view 3d object detection. *arXiv preprint arXiv:2210.02443*, 2022. [2](#), [7](#)
- [41] Bo Peng, Eric Alcaide, Quentin Anthony, Alon Albalak, Samuel Arcadinho, Stella Biderman, Huanqi Cao, Xin Cheng, Michael Chung, Matteo Grella, et al. Rwkv: Reinventing rns for the transformer era. *arXiv preprint arXiv:2305.13048*, 2023. [3](#)
- [42] Jimmy TH Smith, Andrew Warrington, and Scott W Linderman. Simplified state space layers for sequence modeling. *arXiv preprint arXiv:2208.04933*, 2022. [3](#)
- [43] A Vaswani. Attention is all you need. *Advances in Neural Information Processing Systems*, 2017. [1](#), [3](#)
- [44] Jue Wang, Wentao Zhu, Pichao Wang, Xiang Yu, Linda Liu, Mohamed Omar, and Raffay Hamid. Selective structured state-spaces for long-form video understanding. In *Proceedings of the IEEE/CVF Conference on Computer Vision and Pattern Recognition*, pages 6387–6397, 2023. [3](#)
- [45] Shihao Wang, Xiaohui Jiang, and Ying Li. Focal-petr: Embracing foreground for efficient multi-camera 3d object detection. *IEEE Transactions on Intelligent Vehicles*, 2023. [7](#)
- [46] Shihao Wang, Yingfei Liu, Tiancai Wang, Ying Li, and Xiangyu Zhang. Exploring object-centric temporal modeling for efficient multi-view 3d object detection. In *Proceedings of the IEEE/CVF International Conference on Computer Vision*, pages 3621–3631, 2023. [2](#), [3](#), [6](#), [7](#)
- [47] Tai Wang, Xinge Zhu, Jiangmiao Pang, and Dahua Lin. Fcos3d: Fully convolutional one-stage monocular 3d object detection. In *Proceedings of the IEEE/CVF International Conference on Computer Vision*, pages 913–922, 2021. [7](#)
- [48] Yue Wang, Vitor Campagnolo Guizilini, Tianyuan Zhang, Yilun Wang, Hang Zhao, and Justin Solomon. Detr3d: 3d object detection from multi-view images via 3d-to-2d queries. In *Conference on Robot Learning*, pages 180–191. PMLR, 2022. [2](#), [3](#), [7](#)
- [49] Zengran Wang, Chen Min, Zheng Ge, Yinhao Li, Zeming Li, Hongyu Yang, and Di Huang. Sts: Surround-view temporal stereo for multi-view 3d detection. *arXiv preprint arXiv:2208.10145*, 2022. [2](#)
- [50] Zitian Wang, Zehao Huang, Jiahui Fu, Naiyan Wang, and Si Liu. Object as query: Lifting any 2d object detector to 3d detection. In *Proceedings of the IEEE/CVF International Conference on Computer Vision*, pages 3791–3800, 2023. [2](#), [3](#), [7](#)
- [51] Zhuofan Xia, Xuran Pan, Shiji Song, Li Erran Li, and Gao Huang. Vision transformer with deformable attention. In *Proceedings of the IEEE/CVF conference on computer vision and pattern recognition*, pages 4794–4803, 2022. [3](#)
- [52] Yichen Xie, Chenfeng Xu, Marie-Julie Rakotosaona, Patrick Rim, Federico Tombari, Kurt Keutzer, Masayoshi Tomizuka, and Wei Zhan. Sparsefusion: Fusing multi-modal sparse representations for multi-sensor 3d object detection. In *Proceedings of the IEEE/CVF International Conference on Computer Vision*, pages 17591–17602, 2023. [3](#)
- [53] Kaixin Xiong, Shi Gong, Xiaoqing Ye, Xiao Tan, Ji Wan, Errui Ding, Jingdong Wang, and Xiang Bai. Cape: Camera view position embedding for multi-view 3d object detection. In *Proceedings of the IEEE/CVF Conference on Computer Vision and Pattern Recognition*, pages 21570–21579, 2023. [2](#)
- [54] Chenyu Yang, Yuntao Chen, Hao Tian, Chenxin Tao, Xizhou Zhu, Zhaoxiang Zhang, Gao Huang, Hongyang Li, Yu Qiao, Lewei Lu, et al. Bevformer v2: Adapting modern image backbones to bird’s-eye-view recognition via perspective supervision. In *Proceedings of the IEEE/CVF Conference on Computer Vision and Pattern Recognition*, pages 17830–17839, 2023. [7](#)
- [55] Fangao Zeng, Bin Dong, Yuang Zhang, Tiancai Wang, Xiangyu Zhang, and Yichen Wei. Motr: End-to-end multiple-object tracking with transformer. In *European Conference on Computer Vision*, pages 659–675. Springer, 2022. [2](#)
- [56] Xizhou Zhu, Weijie Su, Lewei Lu, Bin Li, Xiaogang Wang, and Jifeng Dai. Deformable detr: Deformable transformers for end-to-end object detection. *arXiv preprint arXiv:2010.04159*, 2020. [3](#)